www.czasopisma.pan.pl PAN POLSKA AKADEMIA NAUK www.journals.pan.pl

Arch. Min. Sci. **65** (2020), 2, 347-361

Electronic version (in color) of this paper is available: http://mining.archives.pl

DOI 10.24425/ams.2020.133197

QIHU WANG[1,2], JIE WANG[1], YICHENG YE[1,3], WEI JIANG[4], NAN YAO[1,3*]

FAILURE CHARACTERISTICS AND STRENGTH MODEL OF COMPOSITE ROCK SAMPLES IN CONTACT ZONE UNDER COMPRESSION

Significant differences in the physical and mechanical properties exist between the rock masses on two sides of an ore-rock contact zone, which the production tunnels of an underground mine must pass through. Compared with a single rock mass, the mechanical behavior of the contact zone composite rock comprising two types of rock is more complex. In order to predict the overall strength of the composite rock with different contact angles, iron ore-marble composite rock sample uniaxial compression tests were conducted. The results showed that composite rock samples with different contact angles failed in two different modes under compression. The strengths of the composite rock samples were lower than those of both the pure iron ore samples and pure marble samples, and were also related to the contact angle. According to the stress-strain relationship of the contact surface in the composite rock sample, there were constraint stresses on the contact surface between the two types of rock medium in the composite rock samples. This stress state could reveal the effect of the constraint stress in the composite rock samples with different contact angles on their strengths. Based on the Mohr-Coulomb criterion, a strength model of the composite rock considering the constraint stress on the contact surface was constructed, which could provide a theoretical basis for stability researches and designs of contact zone tunnels.

Keywords: Contact zone; Composite rock sample; Contact angle; Failure characteristics; Constraint stress; Strength model

[1] SCHOOL OF RESOURCES AND ENVIRONMENTAL ENGINEERING, WUHAN UNIVERSITY OF SCIENCE AND TECHNOLOGY, WUHAN 430081, CHINA
[2] HUBEI KEY LABORATORY FOR EFFICIENT UTILIZATION AND AGGLOMERATION OF MET ALLERGIC MINERAL RESOURCE, WUHAN 430081, CHINA
[3] HUBEI KEY LABORATORY FOR EFFICIENT UTILIZATION AND AGGLOMERATION OF MET ALLERGIC MINERAL RESOURCE, WUHAN 430081, CHINA
[4] DAYE IRON MINE CORPORATION LIMITED OF WISCO RESOURCE GROUP, HUANGSHI, HUBEI 435006, CHINA
* Corresponding author: wang4058113@163.com

1. Introduction

The production tunnels of underground mine must pass through ore-rock contact zone. There are significant differences in the physical and mechanical properties between the rock masses on two sides of an ore-rock contact zone, due to their different diagenesis times, environments, and composition. Additionally, mutual constraints between rock mediums caused by the difference between their deformation characteristics exist on the contact surface under loads. Compared with a single rock mass, the mechanical behavior of a composite rock comprising two rock mediums in the contact zone is more complex (Yassaghi & Salari-Rad, 2005; Mirenkov, 2007, 2009; Krasnovsky, 2019). The practice showed that there were extensive local deformations and collapses in the tunnels through composite rocks, which needed to be applied supports with higher load-bearing capacity (Zhao et al., 2007; Zou et al., 2011; Oliveira et al., 2017; Niedbalski et al., 2018). The poor stability of contact tunnels and the low strength of the surrounding rock near the contact surface are mechanical problems worthy of further discussion. The mechanical behavior characteristics, especially the strength characteristics, of the composite rock mass composed of different rocks under compression is of great significance for revealing the failure mechanism of the contact tunnels.

In studies based on the mechanical properties of composite rock composed of different rock mediums, many experiments have been carried out on layered composite rock composed of salt rock, coal rock, and similar materials. Shah et al. (1985) investigated the stress-strain characteristics of the layered composite rock, and established a relation between strength reduction and the presence of weaker components and the inclined discontinuities in the layered composite rock. Xie et al. (2005) presented the concept of a two-body mechanical model for the interaction between an engineering body and a geological body, and pointed out that the contact effect should be considered between such bodies with different stiffnesses and strengths. Mirenkov (2006) and Krasnovsky (2007) analyzed rock mass deformation near a crack located on an interface of rocks with different properties, and presented a derivation method for systems of singular integral equations for a rock block composed of two uniform parts with a crack. Yang et al. (2005), Li et al. (2006), Liang et al. (2007) and Wang et al. (2010) studied the deformation and failure characteristics of salt rocks with mudstone intercalated under compression and shear, and discussed the effect of the difference in the deformation characteristics between the salt rock and mudstone on the overall deformation and failure characteristics of the layered salt rocks. They also constructed a constitutive model of the interbedded salt rock mass. Nasir et al. (2008) studied the shear stress-strain behaviour and shear strength parameters of the interface between cemented paste backfill (CPB) and rock, and pointed out it was required to develop comprehensive interface models for CPB-rock analyses. Zuo et al. (2013), Huang et al. (2013) and Jie et al. (2015) studied the failure characteristics of coal-rock composite samples and concluded that the existence of weak coal affected the overall failure characteristics and strength of composite samples. Zhao et al. (2014) analyzed the stress state on the strong-weak interface of a three-body model composed of rock and coal with different strengths and stiffnesses, and believed that the additional stresses were derived due to the lateral deformation constraints near the strong-weak interface, which could result in the changes in strength of weak and strong rocks. Liu et al. (2018) established damage constitutive models for coal in a coal-rock combined body, which could reveal the influences of rock on the mechanical behavior of coal in a combined body. Zhang et al. (2018) developed a pseudo-3D model, in which the growth of the planar hydraulic

fracture occurred through multiple horizontal thin coal seams with different elastic properties, to account for the effects of modulus contrasts on fracture shapes. Yin et al. (2017) carried out true triaxial tests on layered composite rock blocks made of fine sandstone, siltstone, and slate, and established a true triaxial strength criterion of layered composite rock based on the modified Lade criterion. Li et al. (2007) established a constitutive model of layered composite rock with soft and hard rock based on Burgers model. Yu et al. (2009) studied the failure characteristics and constitutive relations of a similar model of layered composite rock mass under uniaxial compression. Andjelkovic et al. (2015) and Gutiérrez-Ch et al. (2018) studied the shear behaviour at the contact of concrete-rock mass. Mahmoud et al. (2019) studied the growth of an inclined internal interface crack between two dissimilar rock layers under compression and tension, and found that interface crack growth could occur in stiffer or more compliant layer depending on the elastic stiffness contrast and crack inclination angle.

The contact surfaces of the composite rock mass studied above were nearly horizontal and perpendicular to the external load. However, the rock strata dip angles and the directions of in-situ stress are varied. The mechanical characteristics of the non-horizontal layered composite rock in the contact zone were paid relatively less attention. It was not clear whether the contact angle, which is the angle between the normal of the contact surface and the axial load, would affect the mechanical behavior of composite rock mass. Therefore, the strength characteristics of the composite rock composed of rocks with different strengths and stiffnesses, or different contact angles, are worthy of further research. In order to predict the overall strength of a composite rock, in this paper, the uniaxial compression strengths of iron ore-marble composite rock samples with different contact angles were tested. The failure characteristics of non-horizontal layered composite rock samples and the effect of the contact angle on the overall strength of composite rock samples were discussed. Finally, the strength model of the composite rock considering the constraint stress on the contact surface was constructed, which would provide a theoretical basis for the research of composite rock mass engineering in the contact zone in future.

2. The uniaxial compression test and result analysis

2.1. Sample preparation and test procedure

The contact zone composite rock blocks collected from Daye Iron Mine Corporation Limited of the WISCO Resource Group were selected to process the composite rock samples. In this mine, the contact rock of the ore body was marble, and the boundary between the iron ore with a dark gray color and the marble with a white color was clear, as shown in Fig. 1. The pure iron ore blocks, the pure marble blocks, and the composite rock blocks with approximate plane contact between the iron ore and marble were selected in the mine. By controlling the direction of drilling, the composite rock samples with different contact angles were processed. It was especially ensured that the axis of rock samples was perpendicular to both of the bottoms, which were ground for flatness. Through drilling, cutting and grinding, the cylindrical samples of 100 × 50 mm were obtained. The iron ore and marble each accounted for about half of a sample. The processed standard composite rock samples, as shown in Fig. 2, comprised 8 groups including pure iron ore samples, pure marble samples, and composite rock samples with 6 different contact angles.

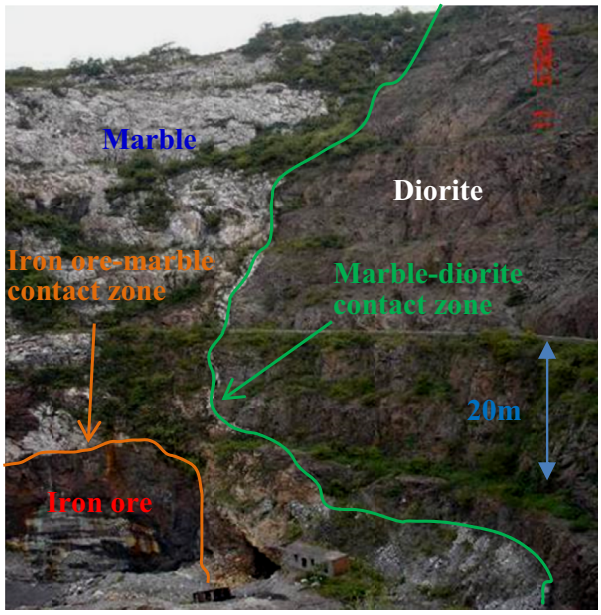

Fig. 1. The iron ore-marble contact zone of the Daye Iron Mine

Uniaxial compression tests of the three kinds of rock sample were carried out on the SAJS-2000 rock press, which can be used to conduct rock uniaxial, triaxial and direct shear tests with maximum force of 2000 kN. A spherical support centering pressing plate was installed in the middle of the upper crossbeam, which could be automatically leveled within 360° to ensure the press plates in close contact with the sample bases. In order to reduce the friction between the sample bases and the press plates, the press plates were first lubricated by oil. With a loading control mode of force control and a loading rate of 0.015 MPa/s, the rock samples were loaded until destruction.

Fig. 2. The standard rock sample in the test

2.2. The failure characteristics of iron ore-marble composite rock samples

The failure characteristics of the iron-marble composite rock samples were affected by the contact angle β. The failure of the composite rock samples with different contact angles showed two different modes.

When the contact angle β was greater than $\beta_c \approx 63.43°$ which is the maximum contact angle when both the upper and lower bottoms were penetrated by the contact surface, the composite rock samples mainly encountered shear failure along the multi-inclined plane. The failure plane was not along the contact surface but entirely in the marble, which was inclined to the sample bottoms and with poor completeness. The iron ore did not fail, and the interface between the iron ore and marble remained intact, as shown in Figs. 3(c) and 3(d).

When the contact angle β was less than β_c, only one rock medium was in contact with the press head, the composite rock samples mainly endured composite failure along a single zigzag surface. In the process of loading, the non-penetrative cracks inclined to the axial were first produced in the marble. Later, sudden failure occurred in the iron ore along the failure plane approximately parallel to the axial, and the composite rock sample completely failed at the same time. In the composite rock samples, shear failure occurred in the marble and tensile failure in the iron ore, both of which were along the same complete failure plane across the interface, as shown in Fig. 3(a) and 3(b).

(a) $\beta \approx 0°$ (b) $\beta \approx 30°$ (c) $\beta \approx 65°$ (d) $\beta \approx 85°$

Fig. 3. The typical failure modes of the iron ore-marble composite rock samples with different contact angles

2.3. The test strengths and failure process analysis

In the three types of rock sample, the pure iron ore samples had the highest strength, with the pure marble samples next, and the composite rock samples had the lowest strength, as shown in Table 1. In uniaxial compression test, the test results will be affected by parallelism and friction of the sample bases. The measures of bases grinding and lubrication were taken to improve the reliability of test results. The average uniaxial compressive strengths of the pure rock samples were closed to those of the test results from Daye Iron Mine (Xu et al. 1999), and also valid.

For the composite rock samples, when the contact angle was less than β_c, the greater the contact angle, the higher the uniaxial compression strength; and when the contact angle was greater than β_c, the uniaxial compression strengths were closed.

TABLE 1

The average uniaxial compressive strength of each rock sample group

Samples	Test strength [MPa]	Lithology
1	112.25	pure iron ore samples
2	51.72	composite rock samples, $\beta \approx 0°$
3	59.91	composite rock samples, $\beta \approx 30°$
4	62.88	composite rock samples, $\beta \approx 45°$
5	68.84	composite rock samples, $\beta \approx 65°$
6	68.78	composite rock samples, $\beta \approx 70°$
7	67.97	composite rock samples, $\beta \approx 85°$
8	71.58	pure marble samples

According to the failure plane distribution, shear failure did not occur along the contact surface in the composite rock sample, indicating that it has a high cohesive strength on the contact surface. Therefore, it can be excluded that the low overall strength of the composite rock sample is caused by the low cohesive strength of the contact surface.

For the composite rock samples with contact angles greater than β_c, due to the high cohesive strength of the contact surface, numerous non-penetrative cracks inclined to the sample bottoms were first produced in the marble with low strength. When the axial load reached the bearing limit of the marble, penetrative failure was produced along some previous non-penetrative cracks in the marble. Under this axial load, the iron ore was not enough to fail.

For the composite rock samples with contact angle less than β_c, numerous non-penetrative cracks inclined to the sample bottoms were also first produced in the marble. When the axial load reached the bearing limit of the marble, at the moment of complete shear failure of the marble, the cohesive force on the failure plane completely disappeared. Due to the constraint of marble, the iron ore not only bore the axial load, but also bore the tensile stress caused by the Poisson effect of the marble. The tensile failure of the iron ore occurred under an axial load below its bearing limit following the failure of the marble.

3. Stress and strain analysis on the contact surface

Under axial stress σ_1, the lateral deformation of the iron ore and marble in the composite rock samples was produced. According to the principle of coordinated deformation of a continuous medium in elastic mechanics, if the contact surface is intact without failure, the lateral strain of the iron ore and marble will remain continuous on the contact surface. Due to the difference in the deformation characteristics between the iron ore and marble, the constraint stress along the contact surface will be produced between the iron ore and marble to maintain the continuous strain of the contact surface.

Therefore, the stress-strain states of the composite rock samples with contact angles greater and less than β_c were analyzed respectively, as shown in Fig. 4.

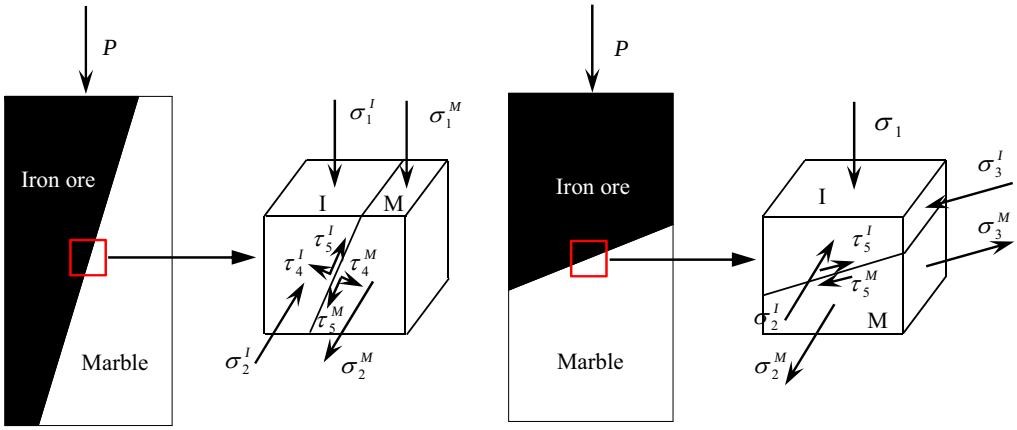

(a) $\beta > \beta_c$ (b) $\beta < \beta_c$

Fig. 4. The stress of microelement at the contact surface of the composite rock

For composite rock samples with contact angles greater than β_c, as shown in Fig. 4(a), the iron ore and marble had the same axial deformation under the axial rigid constraints imposed by the press machine. Therefore, different axial stresses were present in the iron ore σ_1^I and marble σ_1^M, related to the elastic modulus of each rock medium. This stress-strain state of the composite rock samples was similar to that of the roof rock of the tunnel through the contact zone under the action of high strength rigid support. Because the axial surface forces on the upper and lower bottoms of each rock medium were not collinear, stresses τ_4^I, τ_4^M, τ_5^I, and τ_5^M occurred on the contact surface to counteract the couple moment produced by the axial stresses. The magnitude and direction of the resultant force of these contact stresses were equivalent to that of the axial stresses.

Simultaneously, the iron ore and marble should satisfy deformation continuity at the contact surface. In direction 2, parallel to the contact surface, the rock medium with large deformation caused the one with lesser deformation to expand, and the latter, in turn, prevented the former from expanding. From a microcosmic point of view, it can be concluded that there were constraint compressive stress and tensile stress on the contact surface between the two rock mediums with different deformation characteristics. Therefore, according to the deformation continuity condition, the stress-strain relationship on the contact surface of the composite rock should satisfy:

$$\begin{cases} \sigma_1 = \dfrac{\sigma_1^I + \sigma_1^M}{2} \\ \sigma_2^I = -\sigma_2^M \\ \varepsilon_1^I = \varepsilon_1^M \\ \varepsilon_2^I = \varepsilon_2^M \end{cases} \tag{1}$$

where σ_1 is the axial stress of the whole composite rock sample; σ_1^I and σ_1^M are the axial stresses of the iron ore and marble, respectively; σ_2^I and σ_2^M are the constraint stresses between the iron

ore and marble in direction 2 on the contact surface, respectively; ε_1^I and ε_1^M are the axial strains of the iron ore and marble respectively; ε_2^I and ε_2^M are the strains of the iron ore and marble in direction 2 on the contact surface, respectively.

In the uniaxial compression test, iron ore and marble showed approximately linear elastic deformation characteristics, so the iron ore and the marble were assumed to be Hooke's materials for the analysis of stress and strain in the contact zone in this paper. According to Hooke's law, the axial strains and lateral strains of the iron ore and marble are as follows:

$$\begin{cases} \varepsilon_1^I = \dfrac{1}{E_I}(\sigma_1^I - \nu_I \sigma_2^I) \\ \varepsilon_1^M = \dfrac{1}{E_M}(\sigma_1^M - \nu_M \sigma_2^M) \end{cases} \tag{2}$$

$$\begin{cases} \varepsilon_2^I = \dfrac{1}{E_I}(\sigma_2^I - \nu_I \sigma_1^I) \\ \varepsilon_2^M = \dfrac{1}{E_M}(\sigma_2^M - \nu_M \sigma_1^M) \end{cases} \tag{3}$$

Depending on equations (1)~(3), the axial stresses acting on the iron ore and marble can be obtained as follows:

$$\sigma_1^I = \frac{2\left(\dfrac{E_M}{E_I}\nu_I\nu_M + \nu_M^2 - \dfrac{E_M}{E_I} - 1\right)}{\left(\dfrac{E_M}{E_I}\nu_I + \nu_M\right)^2 - \left(\dfrac{E_M}{E_I} + 1\right)^2}\sigma_1 \tag{4}$$

$$\sigma_1^M = \frac{2\left(\dfrac{E_M}{E_I}\nu_I\nu_M + \dfrac{E_M^2}{E_I^2}\nu_I^2 - \dfrac{E_M^2}{E_I^2} - \dfrac{E_M}{E_I}\right)}{\left(\dfrac{E_M}{E_I}\nu_I + \nu_M\right)^2 - \left(\dfrac{E_M}{E_I} + 1\right)^2}\sigma_1 \tag{5}$$

Let:

$$\eta = \frac{2\left(\dfrac{E_M}{E_I}\nu_I\nu_M + \nu_M^2 - \dfrac{E_M}{E_I} - 1\right)}{\left(\dfrac{E_M}{E_I}\nu_I + \nu_M\right)^2 - \left(\dfrac{E_M}{E_I} + 1\right)^2} \tag{6}$$

In this paper, η is defined as the axial stress distribution coefficient of the composite rock sample. η can be used to express the axial stress distribution of two rock mediums with different deformation characteristics in a composite rock sample under compression. Therefore, for

a composite rock sample with a contact angle greater than β_c, the axial stresses of the iron ore and marble can be written simply as follows:

$$\begin{cases} \sigma_1^I = \eta\sigma_1 \\ \sigma_1^M = (2-\eta)\sigma_1 \end{cases} \tag{7}$$

Additionally, the constraint stress of the iron on the contact surface applied by the marble can be expressed as follows:

$$\sigma_2^I = \frac{\frac{E_M}{E_I}\nu_I\eta + \nu_M\eta - 2\nu_M}{\frac{E_M}{E_I}+1}\sigma_1 \tag{8}$$

From which, it can be determined that the constraint stress on the contact surface is proportional to the axial stress of the whole composite rock sample. Let:

$$\lambda_2 = \frac{\frac{E_M}{E_I}\nu_I\eta + \nu_M\eta - 2\nu_M}{\frac{E_M}{E_I}+1} \tag{9}$$

For a composite rock sample with a contact angle greater than β_c, the constraint stress between the iron ore and marble under compression can be written simply as follows:

$$\sigma_2^I = -\sigma_2^M = \lambda_2\sigma_1 \tag{10}$$

where λ_2 is the constraint stress factor of the composite rock sample in direction 2, which is positive for compression and negative for tension.

η and λ_2 are related to the elastic moduli of these two rock mediums, but not to the contact angle. In this paper, according to the mechanical parameters of the iron ore and marble in the Daye Iron Mine, as shown in Table 2, η and λ_2 can be calculated. η was 0.937, indicating that more axial load is applied to the marble, and less to the iron ore. λ_2 was 0.036, showing that the iron ore has constraint compressive stress, and the marble has constraint tensile stress on the contact surface in direction 2.

TABLE 2

The mechanical parameters of the iron ore and marble

Lithology	Elastic modulus [GPa]	Poisson ratio	Internal friction angle [°]	Uniaxial compressive strength [MPa]
Iron ore	15.60	0.27	44	112.25
Marble	18.00	0.20	40	71.58

For composite rock samples with contact angles less than β_c, as shown in Fig. 4(b), both the axial stresses of the iron ore and marble are σ_1 under axial load. σ_1 can be decomposed into

the normal stress σ_4 vertical to the contact surface and the shear stress τ_5 parallel to the contact surface on the contact surface. Due to deformation continuity at the contact surface, there are the constraint stresses on the contact surface in directions 2 and 3, parallel to the contact surface. In this case, the stress-strain relationship on the contact surface of the composite rock should satisfy the following:

$$\begin{cases} \sigma_4 = \sigma_1 \cos^2 \beta \\ \sigma_2^I = -\sigma_2^M \\ \sigma_3^I = -\sigma_3^M \\ \varepsilon_2^I = \varepsilon_2^M \\ \varepsilon_3^I = \varepsilon_3^M \end{cases} \tag{11}$$

where σ_2^I, σ_3^I, σ_2^M, and σ_3^M are the constraint stresses of the iron ore and marble in directions 2 and 3 on the contact surface, respectively; ε_2^I, ε_3^I, ε_2^M, and ε_3^M are the strains of the iron ore and marble in directions 2 and 3 on the contact surface, respectively.

The strains of these two rock mediums in directions 2 and 3 on the contact surface are as follows:

$$\begin{cases} \varepsilon_2^I = \dfrac{1}{E_I}[\sigma_2^I - \nu_I(\sigma_4^I + \sigma_3^I)] \\ \varepsilon_2^M = \dfrac{1}{E_M}[\sigma_2^M - \nu_M(\sigma_4^M + \sigma_3^M)] \end{cases} \tag{12}$$

$$\begin{cases} \varepsilon_3^I = \dfrac{1}{E_I}[\sigma_3^I - \nu_I(\sigma_4^I + \sigma_2^I)] \\ \varepsilon_3^M = \dfrac{1}{E_M}[\sigma_3^M - \nu_M(\sigma_4^M + \sigma_2^M)] \end{cases} \tag{13}$$

Depending on equations (11)~(13), the constraint stress of the iron applied by the marble can be expressed as:

$$\sigma_2^I = \sigma_3^I = \frac{\dfrac{E_M}{E_I}\nu_I - \nu_M}{\dfrac{E_M}{E_I}(1-\nu_I) + (1-\nu_M)} \sigma_1 \cos^2 \beta \tag{14}$$

The constraint stress factors λ_2 and λ_3 in directions of 2 and 3 are:

$$\lambda_2 = \lambda_3 = \frac{\dfrac{E_M}{E_I}\nu_I - \nu_M}{\dfrac{E_M}{E_I}(1-\nu_I) + (1-\nu_M)} \cos^2 \beta \tag{15}$$

Therefore, for a composite rock sample with a contact angle less than β_c, the constraint stresses between the iron ore and marble under compression can be expressed as follows:

$$\begin{cases} \sigma_2^I = -\sigma_2^M = \lambda_2 \sigma_1 \\ \sigma_3^I = -\sigma_3^M = \lambda_3 \sigma_1 \end{cases} \tag{16}$$

Comparing the composite rock samples ($\beta > \beta_c$) with those ($\beta < \beta_c$), the constraint stresses are not only more significant, but also related to the contact angle. In this paper, the constraint stress factors of the iron ore-marble composite rock samples were between 0.01 and 0.07.

4. Strength model of the composite rock considering the constraint stress on the contact surface

According to the result of the stress and strain analysis on the contact surface, under the condition that the contact surface is intact without failure, there will be lateral constraints on the contact surface between the iron ore and marble. In that case, both the iron ore and marble are not in the state of simple uniaxial compression in fact, but there may be compressive stresses or tensile stresses in the other two directions parallel to the contact surface. Therefore, the rock mediums on the contact surface are in the state of biaxial or triaxial force. On the contact surface of the composite rock sample, due to the existence of lateral constraint stress, the compressive capacities of the two rock mediums are not equal to the uniaxial compressive strengths of the corresponding single rock samples. Due to the constraint compressive stress, the compressive capacity of the iron ore is higher than that of the pure iron ore samples. And due to the constraint tensile stress, the compressive capacity of the marble was less than that of pure marble samples. In this paper, it is assumed that the overall strength of the composite rock sample could be expressed by the strength of the weak rock medium in it. In the iron-marble composite rock samples, the compressive capacity of the marble with low strength is weakened, and the compressive strength of the iron ore with high strength is strengthened. As a result, the overall strength of the iron ore-marble composite rock sample was lower than that of the pure iron ore sample and pure marble sample. However, for the composite rock samples with contact angles greater than β_c, more axial stress was applied to the marble with a relatively high stiffness and low strength. Therefore, the difference in the deformation characteristics between the iron ore and marble in the iron ore-marble composite rock samples can weaken its overall strength.

The composite rock samples with contact angles greater than β_c are constrained in only one direction and not obviously on the contact surface. So, in this paper, the effect of the lateral constraint stress on the overall strength of the composite rock samples with contact angles less than β_c was predominantly discussed. The lateral constraint stresses σ_2 and σ_3 in two directions along the contact surface can be decomposed into the horizontal constraint stresses σ_{h1} and σ_{h2}, in which:

$$\begin{cases} \sigma_{h1} = \sigma_2 = \pm\lambda_2 \sigma_1 \\ \sigma_{h2} = \sigma_3 \cos\beta = \pm\lambda_3 \sigma_1 \cos\beta \end{cases} \tag{17}$$

Considering that the σ_{h1} and σ_{h2} are not equal, the method of Bhawani (1998) can be referred to deal with the intermediate principal stress. The average values of σ_{h1} and σ_{h2} can be introduced

into the Mohr-Coulomb strength criterion instead of the third principal stress. The strength model of the rock mediums on the contact surface was constructed as follows:

$$\sigma_1 = \frac{K(\sigma_{h1} + \sigma_{h2})}{2} + \sigma_c \tag{18}$$

where $K = \dfrac{1+\sin\phi}{1-\sin\phi}$, and φ is the angle of internal friction of the rock.

Depending on equations (17) and (18), the relationship between the axial bearing limit of each rock medium on the contact surface in the composite rock and its uniaxial compressive strength can be written as follows:

$$\sigma_1 = \chi\sigma_c \tag{19}$$

where $\chi = \dfrac{2}{2 \pm K(\lambda_2 + \lambda_3 \cos\beta)}$, defined as the strength factor of the composite rock to express the effect of the difference in the deformation characteristics between the two rock mediums in the composite rock on their strengths.

In the composite rock samples with contact angles greater than β_c, the constraint stress on the contact surface is relatively small. we can assume that the composite rock sample would be destroyed when the axial stress distributed on each rock medium reaches its uniaxial compressive strength.

Therefore, considering the constraint stress on the contact surface, the strength model of the composite rock samples in the contact zone comprising the two rock mediums A and B is as follows:

$$\sigma_c^{AB} = \begin{cases} \min(\chi_A \sigma_c^A, \chi_B \sigma_c^B), \beta \le \beta_c \\ \min\left(\dfrac{\sigma_c^A}{\eta}, \dfrac{\sigma_c^B}{2-\eta}\right), \beta > \beta_c \end{cases} \tag{20}$$

where $\sigma AB\ c$, $\sigma A\ c$, and $\sigma B\ c$ are the uniaxial compressive strengths of the composite rock, rock A and rock B, respectively; η is the axial stress distribution coefficient of the composite rock; χ_A and χ_B are the strength factors of rock A and rock B, respectively.

5. Verification of the strength model

Fig. 5 shows a comparison between the uniaxial compressive strength test values of the iron ore-marble composite rock samples and the prediction curve of the strength model. The strength model can not only describe the variation law of the strength test values of the composite rock samples with different contact angles under compression, but also accurately fits the test values with errors ranging from 0.4% ~ 5.5%. Excluding the composite rock sample with a contact angle of 0°, the strength test values of the others do not differ significantly from the predicted values of the strength model. The authors thought that the errors might be mainly caused by the heterogeneity of iron ore especially in the composite rock samples with a contact angle of 0°,

which contained some marble impurities. On the whole, this strength model is valid without obvious error.

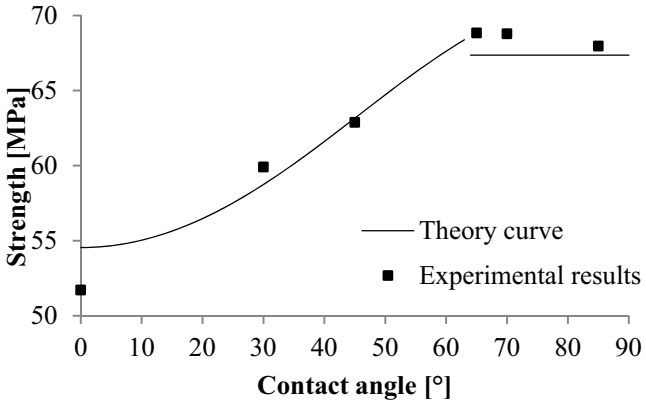

Fig. 5. The comparison between experimental results and theory curve for composite rock sample strengths

6. Conclusions

In this paper, by the uniaxial compression tests and the stress-strain analysis on the contact surface, the effect of the difference in the deformation characteristics of the composite rock sample on its overall strength was analyzed. Then the strength model of the composite rock was constructed to predict the overall strength of the composite rock with different contact angles. The following statements can be concluded:

(1) Under the axial load lower than the uniaxial compressive strength of marble, the marble in the iron ore-marble composite rock sample initially failed, which led to the whole failure of the composite rock sample. The overall strengths of the iron ore-marble composite rock samples are lower than those of the pure rock samples, and related to the contact angle.

(2) Due to the difference of the deformation characteristics, the constraint compression stress and tensile stress exist on the contact surface in the composite rock sample under compression. As a result, the compressive capacity of each rock medium is not equal to its uniaxial compressive strength.

(3) Considering the constraint stress on the contact surface in the composite rock sample, based on the Mohr-Coulomb strength criterion, the strength model of the composite rock in the contact zone was constructed. With this model, the predicted strength values are in good agreement with the test values. The overall strength of the composite rock with different strengths, stiffnesses, and contact angles in the contact zone can be predicted, as the basic data for the stability researches and designs of contact zone tunnels.

The results of both the uniaxial compression tests and the theoretical analysis show that the compressive capacity of the rock near the contact surface may be weakened. In the stability analysis of tunnel engineering through the ore-rock contact zone, no matter which kind of fail-

ure criterion is used, consideration of the weakening of the compressive capacity of rock near the contact surface should be highly advised. According to the strength factor of the composite rock in the contact zone, the rock strength values near the contact surface should be reduced correspondingly.

Rock is a nontensile medium, so for composite rock with a significant difference in the deformation characteristics, the constraint tensile stress on the contact surface may lead directly to the tensile failure of rock near the contact surface under a certain load. In this case, the failure characteristics and strength model of the composite rock are worthy of further discussion.

The mathematical model for the analysis of stress and strain in the contact zone was based on the assumption that both materials the iron ore and the marble were Hooke's materials, so the strength model is suitable for the composite rock samples comprising hard rock mediums with approximately linear elastic deformation characteristics. It is also necessary to further study the strength model of composite rock samples consider the nonlinear elastic deformation and plastic deformation.

Acknowledgments

This study was supported by the National Natural Science Foundation of China (Nos. 51704213 and 51574183), Natural Science Foundation of Hubei Province (No. 2017CFC831). We would like to thank Editage [www.editage.cn] for English language editing.

References

Andjelkovic V., Pavlovic N., Lazarevic Z., Nedovic V., 2015. *Modelling of shear characteristics at the concrete-rock mass interface*. International Journal of Rock Mechanics and Mining Sciences **76**, 222-236.

Bhawani S., Goel R.K., Mehrotra V.K., Garg S.K., Allu M.R., 1998. *Effect of intermediate principal stress on strength of anisotropic rock mass*. Tunneling and Underground Space Technology **13** (1), 71-79.

Gutiérrez-Ch J.G., Senent S., Melentijevic S., Jimenez R., 2018. *Distinct element method simulations of rock-concrete interfaces under different boundary conditions*. Engineering Geology **205**, 123-139.

Huang B., Jiangwei L., 2013. *The effect of loading rate on the behavior of samples composed of coal and rock*. International Journal of Rock Mechanics and Mining Sciences **61**, 23-30.

Jie L., Enyuan W., Dazhao S., Siheng W., 2015. *Effect of rock strength on failure mode and mechanical behavior of composite samples*. Arabian Journal of Geosciences **8** (7), 4527-4539.

Krasnovskii A.A., Mirenkov V.E., 2007. *Analysis of deformation of the compound rock blocks with cracks*. Journal of Mining Science **43**, 132-144.

Krasnovsky A.A., 2019. *Strength of inhomogeneous rib pillars*. IOP Conference Series: Earth and Environmental Science **262**, 012037.

Li W., Li X., Han B., Shu Y., 2007. *Recognition of creep model of layer composite rock mass and its application*. Journal of Central South University of Technology **14** (1), 329-331.

Li Y., Liu J., Yang C., 2006. *Influence of mudstone interlayer on deformation and failure characteristics of salt rock*. Chinese Journal of Rock Mechanics and Engineering **25** (12), 2461-2466.

Liang W., Yang C., Zhao Y., Dusseault M.B., Liu J., 2007. *Experimental investigation of mechanical properties of bedded salt rock*. Journal of Rock Mechanics and Mining Sciences **44** (3), 400-411.

Liu X.S., Tan Y.L., Ning J.G., Lu Y.W., Gu Q.H., 2018. *Mechanical properties and damage constitutive model of coal in coal-rock combined body*. International Journal of Rock Mechanics and Mining Sciences **110**, 140-150.

Mahmoud A., Mahmoud B., Raheb B., 2019. *Analytical investigations of interface crack growth between two dissimilar rock layers under compression and tension*. Engineering Geology **259**, 105188.

Mirenkov V.E., 2006. *Rock mass deformation near a crack located on an interface of rocks with different properties*. Journal of Mining Science **42**, 315-321.

Mirenkov V.E., 2007. *Contact problems in rock mechanics*. Journal of Mining Science **43** (4), 370-381.

Mirenkov V.E., 2009. *On probable failure of an undercut rock mass*. Journal of Mining Science **45**, 105-111.

Nasir O., Fall M., 2008. *Shear behaviour of cemented pastefill-rock interfaces*. Engineering Geology **101**, 146-153.

Niedbalski Z., Małkowski P., Majcherczyk T., 2018. *Application of the NATM method in the road tunneling works in difficult geological conditions – The Carpathian flysch*. Tunnelling and Underground Space Technology **74**, 41-59.

Oliveira D., Diederichs M.S., 2017. *Tunnel support for stress induced failures in Hawkesbury Sandstone*. Tunnelling and Underground Space Technology **64**, 10-23.

Shah S.D., Parthasarathy A., Limaye R.C., 1985. *Geomechanical model simulation for the varied rock formations of the Kadana dam foundation, Gujarat, India*. Bulletin of the International Association of Engineering Geology **31**, 123-129.

Wang A., Li X., Yang C., Huang Z., 2010. *Study of interaction between creep deformation of bedded salt rock*. Rock and Soil Mechanics **31** (12), 3964-3970.

Xie H., Chen Z., Zhou H., Yi C., Chen Z., 2005. *Study on two-body mechanical model based on interaction between structural body and geo-body*. Chinese Journal of Rock Mechanics and Engineering **24** (9), 1457-1464.

Xu D., Chen C., Xu Y. Ren W., Gu X., 1999. *A Study of the Rock Mechanical Parameters of Slopes in East Open-pit Stope of Daye Iron Mine*. Rock and Soil Mechanics **20** (4), 69-75.

Yang C., Li Y., 2005. *Expanded cosserat medium constitutive model for laminated salt rock*. Chinese Journal of Rock Mechanics and Engineering **24** (23), 4226-4232.

Yassaghi A., Salari-Rad H., 2005. *Squeezing rock conditions at an igneous contact zone in the Taloun tunnels, Tehran-Shomal freeway, Iran: a case study*. International Journal of Rock Mechanics and Mining Sciences **42** (1), 95-208.

Yin G., Li X., Lu J., Song Z., 2017. *A failure criterion for layered composite rock under true triaxial stress conditions*. Chinese Journal of Rock Mechanics and Engineering **36** (02), 261-269.

Yu Y., Hu M., Yang X., Liang W., 2009. *Similarity simulation of bedded composite rock*. Metal Mine **1**, 21-24.

Zhang X., Wu B., Connell L.D., Han, Y., Jeffrey R.G., 2018. *A model for hydraulic fracture growth across multiple elastic layers*. Journal of Petroleum Science and Engineering **167**, 918-928.

Zhao X., Tang C., Tian J., 2007. *Study on evolvement law of background stress field of multi-step excavation of roadway*. Rock and Soil Mechanics **28** (4), 659-662.

Zhao Z., Wang W., Dai C., Yan J., 2014. *Failure characteristics of three-body model composed of rock and coal with different strength and stiffness*. Transactions of Nonferrous Metals Society of China **5**, 1538-1546.

Zou C., Ye Y., Wang W., Wang S., Jing H., 2011. *Monitoring analysis on deformation of the roadway bolting by GFRP of Jinshandian iron mine*. Metal Mine (11), 41-44.

Zuo J., Wang Z., Zhou H., Pei J., Liu J., 2013. *Failure behavior of a rock-coal-rock combined body with a weak coal interlayer*. International Journal of Mining Science and Technology **23** (6), 907-912.